

# Fabrication, Characterization, and Application in SERS of Self-Assembled Polyelectrolyte–Gold Nanorod Multilayered Films

Xiaoge Hu, Wenlong Cheng, Tie Wang, Yuling Wang, Erkang Wang,\* and Shaojun Dong\*

State Key Laboratory of Electroanalytical Chemistry, Changchun Institute of Applied Chemistry, Chinese Academy of Sciences, Graduate School of the Chinese Academy of Science, Changchun, Jilin 130022, China

Received: May 23, 2005; In Final Form: August 10, 2005

An effective and facile approach for the preparation of multilayered nanostructure of gold nanorods (Au NRs) has been demonstrated. Linear polyethylenimine (LPEI) was selected as a polymeric adhesive layer, and an anionic polyelectrolyte poly(sodium styrenesulfonate) (PSS) was used as the linker of the positively charged Au NRs in multilayered nanostructure. They were deposited onto the LPEI-modified indium-doped tin oxide (ITO) substrate alternately using the layer-by-layer assembly technique via electrostatic interactions. The plasmonic property of the multilayered nanostructure of Au NRs is tunable by the controlled self-assembly process. FE-SEM was used to study the morphologies of the resulted substrates with Au NRs monolayer membrane and with Au NRs multilayered membrane. More importantly, it was found that the multilayered NRs films could be used as a surface-enhanced Raman spectroscopy (SERS) substrate for probing 4-aminothiophenol (4-ATP).

## 1. Introduction

There has been a growing interest in synthesis and characterization of metal nanoparticles (NPs) with variable size and shape due to their geometry-dependent unique optical, electronic, and catalytic properties.<sup>1–3</sup> These distinct properties may be attributed to the quantum confinement phenomena derived from the change in the density of the electronic energy level as well as a high ratio of surface to bulk atoms.<sup>4</sup>

Rodlike metal nanoparticles are of great interest due to their novel optical and chemistry properties<sup>5–11</sup> such as two separated plasmon resonance bands,<sup>5–7</sup> strong surface-enhanced Raman scattering (SERS),<sup>8,9</sup> fluorescence,<sup>10</sup> and anisotropic chemical reactivity,<sup>11</sup> which might be of significance for the applications in future nanoelectronics and nanodevices. The miniaturization of electronic devices has attracted more and more interest recently.<sup>12–14</sup> The bottom-up approach is a feasible way to fabricate much smaller devices where devices are self-assembled from small building blocks. Considerable efforts have been directed to assemble the low-dimensional building blocks into two-dimensional (2D) and three-dimensional (3D) nanoconstructions.<sup>15–22</sup> El-Sayed et al.<sup>15</sup> have organized Au NRs into one-, two-, and three-dimensional structures by controlling the evaporation of solvent. Mallouk and co-workers<sup>16,17</sup> have selectively assembled the gold nanowires onto Au films using deoxyribonucleic acid (DNA) chemistry. In general, DNA-derivatized nanowires were immobilized on Au films modified with DNA oligonucleotides complementary to that of the nanowires. Except for a microfluidic-based approach,<sup>18</sup> which has been used to align nanowires, the Langmuir–Blodgett technique is a versatile and powerful approach for the assembly of anisotropic building blocks in large area.<sup>19–22</sup> Murphy et al.<sup>23</sup> have demonstrated that electrostatic interactions lead to the organization of Au NRs onto self-assembled monolayers (SAMs). Whereas, the application of these building blocks in

nanodevices needs well control on the assembly process, moreover, assemblies of the nanomaterials on transparent substrates offer advantage in investigating their optical properties. To solve these problems, the layer-by-layer (LBL) technique is an excellent choice. Recently, the electrostatic LBL deposition of oppositely charged polyelectrolytes,<sup>24</sup> DNA,<sup>25</sup> conducting polymers,<sup>26</sup> proteins,<sup>27</sup> and metal or semiconductor nanoparticles<sup>28</sup> is widely used to fabricate ordered and functional membrane. LBL assembly affords nanoscale control over the internal architecture. Polyelectrolytes are extraordinarily attractive to be used as the “glue molecule” in the construction of multilayers of charged metal nanoparticles with multifunctional nanostructured materials.<sup>29,30</sup> The as-prepared metal nanoparticle multilayer structures are optically and electrically approachable, showing interesting photoelectrochemistry<sup>31</sup> and sensing<sup>32</sup> properties. Up to now, it is scarcely seen that the Au NRs nanocomposite materials were fabricated by the LBL technique. In this article, we have first constructed Au NRs multilayer films through LBL assembly of poly(sodium styrenesulfonate) (PSS) and positively charged Au NRs on linear polyethylenimine (LPEI)-derivatized indium-doped tin oxide (ITO) substrate. The coverage of Au NRs is increased with increasing of the number of deposition layer. The UV–vis absorbance spectrum and SEM were used to characterize the multilayered membrane. The as-prepared Au NRs multilayered membranes also have application in surface-enhanced Raman scattering spectrum analysis. Strong SERS signal for probe molecule 4-aminothiophenol (4-ATP) indicates that the membrane is an active SERS substrate. Thus-prepared multilayered structures are desired to have wide potential application in nanodevices and single molecule detection.

## 2. Experimental Section

**Reagents and Materials.** Hydrogen tetrachloroaurate(III) trihydrate ( $\text{HAuCl}_4 \cdot 3\text{H}_2\text{O}$ , 99.9%), hexadecyltrimethylammonium bromide (CTAB, 98%), PSS ( $M_w = 70\,000$ ), and LPEI ( $M_n = 423$ ) were purchased from Aldrich. Vitamin C (99.5%)

\* To whom correspondence should be addressed: Fax +86-431-5689711; e-mail ekwangaciac.il.cn or dongsj@ciac.jl.cn.

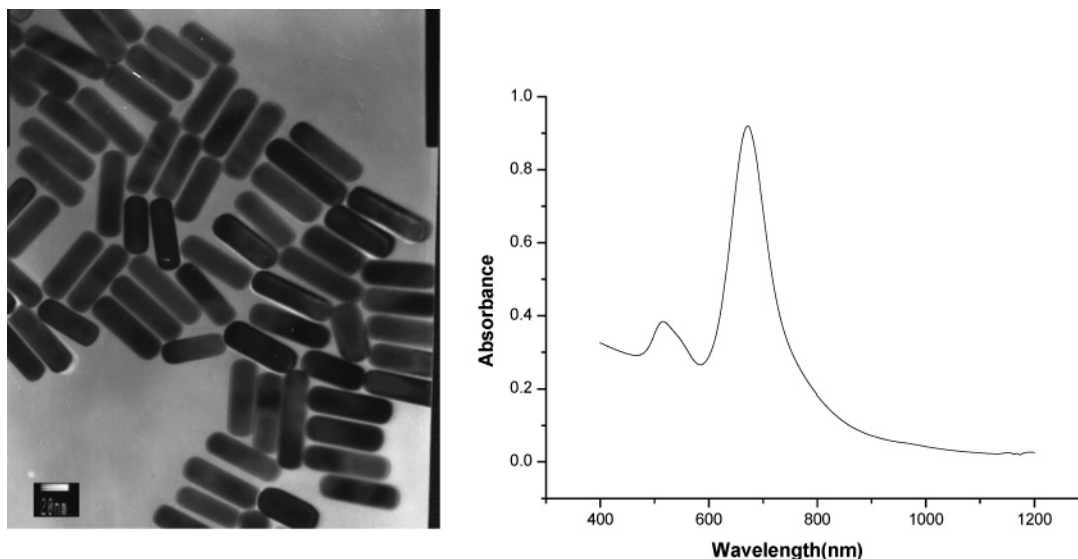


**Figure 1.** A typical TEM image of gold nanorods with aspect ratio 3. Scale bar is 20 nm. The UV-vis spectrum of the Au NRs dispersing in water was also shown (right).

was obtained from Fluck. Sodium borohydride ( $\text{NaBH}_4$ , 99%) and 4-ATP were obtained from ACROS. All chemicals were used without further purification. Ultrapure water purified with Milli-Q plus system (Millipore Co.) was exclusively used in all aqueous solutions and rinsing procedures. Its resistivity was over  $18 \text{ M}\Omega\cdot\text{cm}$ . ITO glass was purchased from Changchun Institute of Optics and Mechanics with a square resistance of  $80 \Omega\cdot\text{cm}^{-2}$ .

**Preparation of Gold Nanorods.** All glassware used in the following procedures was cleaned in a bath of freshly prepared 3:1  $\text{HCl}/\text{HNO}_3$  and rinsed thoroughly in  $\text{H}_2\text{O}$  prior to use. Surfactant-capped Au NRs with a plasmon coupling band at 685 nm were prepared using a modified version<sup>33</sup> of the seed-mediated<sup>34–36</sup> growth method. Briefly, CTAB-capped 4 nm gold nanoparticles were synthesized by chemical reduction of  $\text{HAuCl}_4$  with  $\text{NaBH}_4$  in water. The gold spheres served as seeds on which to grow rodlike gold nanoparticles. The seeds then were added to the growth solution containing more  $\text{HAuCl}_4$ , rodlike micelle CTAB, and a weak reducing agent Vitamin C. Au NRs could be formed in several minutes. The aspect ratio of the as-prepared NRs can be controlled by the ratio of gold seeds to gold salt in the solution. After preparation, excess surfactant was removed from the nanoparticles by centrifuging the solution at 6000 rpm for 12 min. The precipitation was collected and redispersed in deionized water. Samples were prepared for TEM studies by drop-casting one drop of the NRs solution on a carbon-coated copper grid and evaporating the solution at room temperature.

**Layer-by-Layer Assembly of Oppositely Charged Au NRs and Polyelectrolyte.** ITO conducting glass was thoroughly cleaned according to the literature.<sup>37</sup> Briefly, ITO glass slides with  $1.0 \text{ cm} \times 5.0 \text{ cm}$  dimensions were sonicated for 15 min in each of the following solvents—soapy water, water, chloroform, and neat acetone—and then immersed in saturated  $\text{NaOH}$  aqueous solution for several minutes. After being thoroughly rinsed by water and dried under a stream of nitrogen, the ITO slides were orderly immersed into 10 mM LPEI aqueous solution (containing 0.2 M  $\text{NaCl}$ ) and 10 mM PSS aqueous solution (containing 0.2 M  $\text{NaCl}$ ) for 2 h each. After exhaustive rinsing by water and drying by nitrogen, the substrate was immersed in concentrated Au NRs solution for 12 h. This is the first layer of Au NRs, and the subsequent bilayers of PSS/Au rods were deposited onto the substrate by sequential immersion of the substrate into PSS aqueous solution for 20

min and the as-prepared Au NRs solution for 40 min. The above two steps were repeated alternatively until the desired number of layers was obtained.

**FE-SEM Characterization and SERS Activity.** The ITO conductive glass slides with one Au NRs layer and with 11 Au NRs layers were cut into  $1.0 \text{ cm} \times 1.0 \text{ cm}$  slides and then imaged directly by field emission scanning electron microscopy (FE-SEM) without any metallic coating. As for SERS measurement, the ITO glass slides with various Au NRs layers were cut into  $1.0 \text{ cm} \times 1.0 \text{ cm}$  slides and then immersed in  $1.0 \times 10^{-6} \text{ M}$  4-ATP solution for several hours. After thoroughly rinsing with water and drying by nitrogen, they were subjected to Raman characterization by a FT-Raman spectrometer.

**Instrumentation.** Optical spectra were acquired using Cary 500 UV-vis NTR spectrometer (Varian). Transmission electron microscopy (TEM) samples were examined by using a JEOL 2010 TEM operating at 200 kV. The conductive ITO film with attached Au NRs was measured by using XL30 ESEM FEG field emission scanning electron microscopy (FE-SEM) (FEI Co.) at an accelerating voltage of 20 kV. The Raman instrument includes a FT-Raman spectrometer (Thermo Nicolet 960) equipped with an InGaAs detector and a Nd:VO<sub>4</sub> laser (1064 nm) as an excitation source. The laser power used was about 400 mW. All FT-SERS were recorded by averaging 1024 scans.

### 3. Results and Discussion

**Gold Nanorods Formation.** The Au NRs obtained were characterized by TEM and UV-vis spectroscopy. A representative TEM image is shown in Figure 1 (the left image). The gold nanorods are quite uniform in shape and size. The average length and aspect ratio is 60 nm and 3, respectively. The heavy capping of CTAB on the surface of Au NRs kept them well separated. The right image in Figure 1 shows the UV-vis spectrum measured from the Au NRs dispersing in water. The spectrum exhibits two distinct plasmon absorption bands centered at 520 and 685 nm. The first absorption band is assigned to the transverse plasmon resonance band of gold NRs, and the gold nanoparticles also give some contributions to this absorption band. The other one located at longer wavelength band is the longitudinal plasmon resonance band of Au NRs. The adsorption bands are quite narrow, indicating the monodispersity of Au NRs.

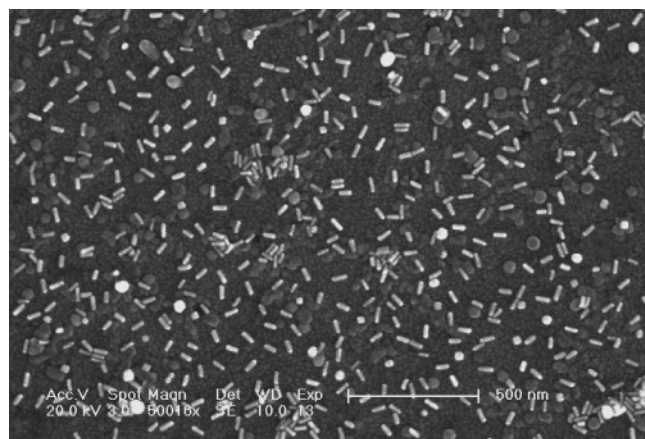


**Figure 2.** Typical SEM image of a monolayer Au NRs assembled on LPEI-derivatized ITO substrate.

**Formation and Characterization of the Monolayer and Multilayer Films. (1). The Monolayer Film of Au NRs.** The monolayer film of Au NRs was prepared by a wet chemical assembly strategy through the electrostatic interaction. The cationic polyelectrolyte LPEI was used as an adhesive layer for the assembly of Au NRs. It is well-known that the Au NRs capped by a bilayer of CTAB are positively charged;<sup>38</sup> therefore, the connection of the PEI-modified substrate with Au NRs via a negatively charged anionic polyelectrolyte PSS is indispensable. After the ITO substrate was modified with LPEI, subsequent immersion into PSS and Au NRs solution results in the deposition of the first layer of Au NRs on the substrate. The morphology of the deposited monolayer structure was studied by FE-SEM. Figure 2 shows a typical FE-SEM image of the as-prepared Au NRs monolayer film. The bright images correspond to Au NRs, which are evenly distributed on the substrate. Most of the NRs exist separately, but a few aggregates consisting of several NRs are also observed.

**(2) The Multilayer Film of Au NRs.** The preparation of the multilayer film of Au NRs is based on the layer-by-layer assembly approach, i.e., the use of oppositely charged species for an alternate deposition onto a flat substrate.<sup>39</sup> Murphy et al.<sup>40</sup> have recently demonstrated that alternate adsorption of anionic and cationic polyelectrolytes on positively charged Au NRs leads to the formation of polyelectrolyte multilayers around the nanorods. The electrostatic attractive interactions between the negatively charged PSS and CTAB-capped Au NRs are strong enough to drive the formation of multilayered nanostructure of Au NRs on substrate.<sup>41–43</sup> The formation of multilayered nanostructure of Au NRs can be distinctly described by the following schematic figure (Scheme 1). First, an ITO substrate was modified with a layer of positively charged polyelectrolyte LPEI, and the subsequent treating with negatively charged PSS resulted in a negative surface. Au NRs are positively charged because of the heavy capping of cationic surfactant CTAB on gold surfaces.<sup>38,40</sup> So Au NRs can easily self-assemble onto the negative surface via strong electrostatic interaction to generate the first layer of Au NRs. In the subsequent assembly process, the negatively charged PSS was used as an LBL partner macromolecule for the Au NRs. Repeatedly depositions of PSS and Au NRs on the Au NRs monolayer result in the formation of Au NRs multilayer film on the substrate. The LBL assembly process was monitored by UV–vis absorbance spectra on-line. After each successive adsorption of PSS aqueous solution for 20 min and Au NRs for 40 min, the absorbance spectrum of the resulted ITO substrate was recorded. The UV–vis absorbance spectra of seven layers of Au NRs formed by LBL

**SCHEME 1: Schematic Representation of the Formation Process of Multilayered Au NRs Membrane through the LBL Assembly Approach**

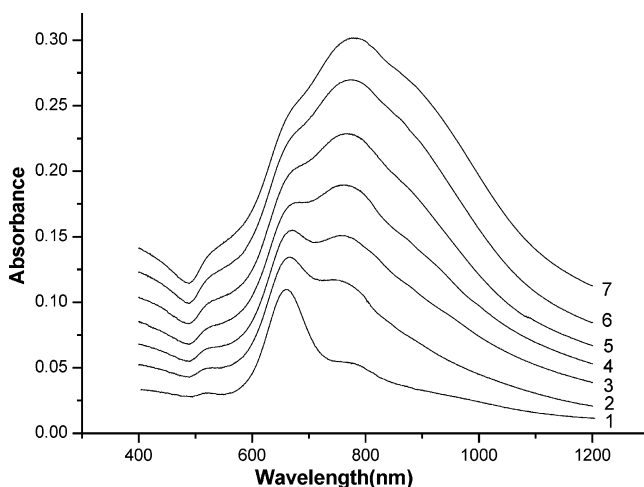
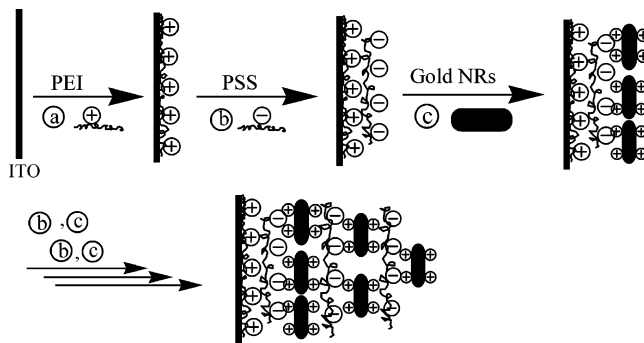


**Figure 3.** UV–vis absorbance spectral monitoring of growing process of multilayered films with seven layers of Au NRs. The layer numbers are marked beside each curve.

assembly are shown in Figure 3. The buildup of multilayered NRs structure was demonstrated by the increase in Au NRs surface plasmon band located at 518 and 660 nm. Importantly, a new red-shifted absorption band around 770 nm was also observed and the absorbance was more and more strong. This new band at 770 nm is attributed to the strong electromagnetic coupling between neighboring NRs, which can be supported by the extensive literature on the dependence of surface plasmon band on interparticle separation.<sup>39,44–46</sup> With increasing of NRs deposition the coupling interaction becomes more extensive to result in the increase of peak intensity. Interestingly, the plasmon absorption band at 660 nm corresponding to the longitudinal plasmon resonance of Au NRs on substrate is slightly blue-shifted relative to that of the Au NRs in solution at 685 nm. This is consisted with the result of El-Sayed et al. that the plasmon maximum of the dried films blue-shifts relative to that of the NRs in solution.<sup>9</sup> In addition, the NRs are piled up closely, and therefore the medium dielectric constant is different from that of the nanorods dispersion.<sup>47</sup>

The resulted multilayered Au NRs structure has been subjected to FE-SEM characterization, as shown in Figure 4. Apparently, the Au NRs are thickly and closely packed on the whole surface, and the coverage density is extremely high, except for some small areas are not covered with NRs. To obtain the clear morphological information on the NRs multilayered nanostructure, we imaged the morphologies of multilayer on conductive ITO without using any metallic coating and the multilayer films were connected to the sample support by a piece



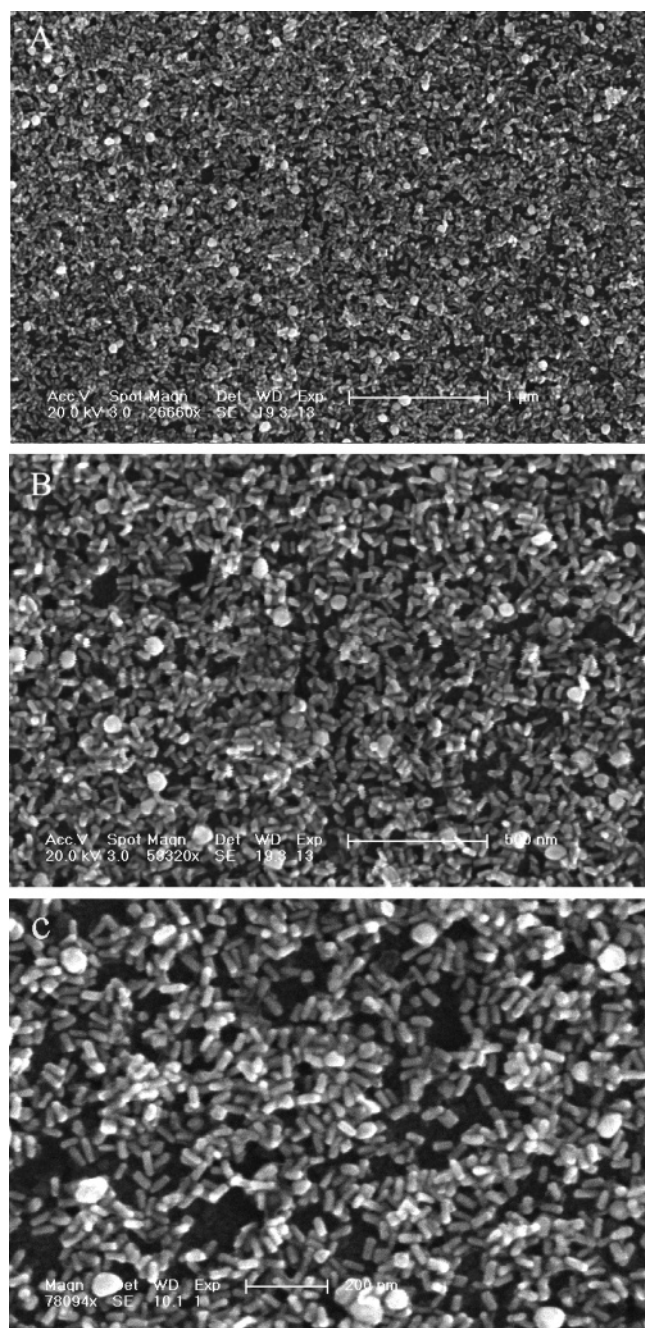


**Figure 4.** Typical FE-SEM images of Au NRs multilayer film assembled on the LPEI-derivatized ITO substrate. Images A, B, and C are taken from the same membrane at different magnifications. Scale bar is 1  $\mu\text{m}$ , 500 nm, and 200 nm, respectively.

of conductive adhesive tape. Parts A–C of Figure 4 are images taken from different magnifications.

The Au NRs are still independent in the close-packed multilayer films without agglomeration. Small quantities of bright spherical particles are also observed around the Au NRs on the substrate. They were demonstrated by energy-disperse X-ray (EDX) to be gold NPs, which are hard to be thoroughly separated from NRs by centrifugation. Similar NPs were also observed from TEM experiments, which were not shown in the article. This strategy shows several advantages comparing with direct modification on solution-state NRs, such as the aggregation of NRs can be avoided, and the as-prepared multilayer films are extremely stable and accessible to optical investigation. Besides, the coverage of Au NRs on the film can be tuned

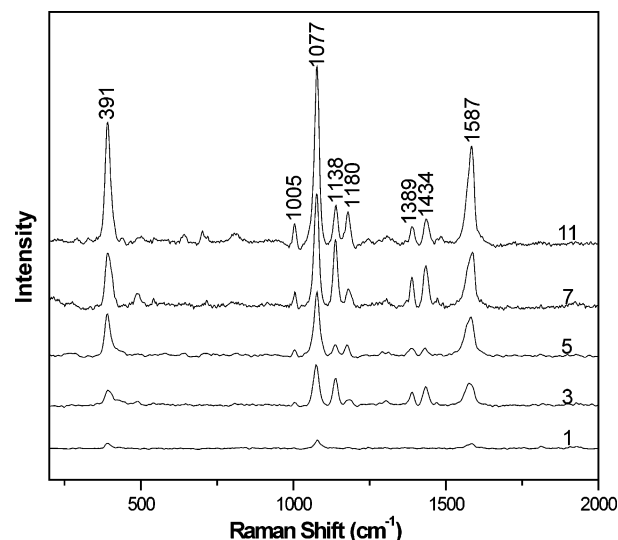


**Figure 5.** FT-SERS spectra of 4-ATP ( $1 \times 10^{-6}$  M) absorbed on the surfaces of gold multilayer films with various Au NRs layers. The layer numbers are marked beside each curve.

through varying the concentration of NRs solution, the immersion time of the substrate in NRs solution, and the numbers of the PSS/Au bilayers deposited on the substrate. In addition, the large-scale and high-density NRs assemblies described here have high reproducibility, enabling and facilitating the fabrication of nanoscale interconnects.<sup>20,48</sup>

**SERS Spectra of 4-ATP on the Substrates with Various Au NRs Layers.** It has been demonstrated that the formation of aggregates of metal nanoparticles induce stronger SERS enhancement.<sup>49–53</sup> The closely contacted Au NRs possess possible SERS active sites at their junctions.<sup>9</sup> According to these theoretical and experimental studies, the high-density NRs multilayer film presented here was expected to have high local electromagnetic (EM) field enhancement and could be served as SERS substrates for molecular sensing. We investigated the SERS intensity of the adsorbate on the surface of above-mentioned Au NRs multilayer films. 4-ATP was selected as the probing molecule. To investigate the impact of the increasing gold layers on the SERS enhancement, SERS spectra of 4-ATP were collected at different substrates with various Au NRs layers. Figure 5 shows a set of FT-SERS spectra of 4-ATP on the surfaces of Au NRs multilayer films containing various NRs layers. As indicated in the figure, the SERS signal intensities increase with the increase of Au NR layers. This is attributed to the facts that increased numbers of Au NRs result in the increased active sites and enhanced local electromagnetic field. The spectra are dominated with the  $a_1$  vibration modes (in-plane, in-phase modes), such as  $\nu(\text{CC})$  at  $1587 \text{ cm}^{-1}$  and  $\nu(\text{CS})$  at  $1077 \text{ cm}^{-1}$ . The band at  $391 \text{ cm}^{-1}$  is assigned to one of the vibration modes of the C–S bond, most likely the bending mode of the C–S bond.<sup>54,55</sup>

It is noteworthy that the  $b_2$  modes (in-plane, out-of-phase modes) located at  $1434$ ,  $1389$ , and  $1138 \text{ cm}^{-1}$  are also apparently enhanced, even though there is a slight frequency shift relative to the literature. The apparent enhancement of the  $b_2$  modes has been ascribed to the charge transfer (CT) of the metal to the adsorbed molecules.<sup>54–57</sup> The predominance of  $a_1$  modes in the FT-SERS spectra (Figure 5) may imply that the enhancement via an EM mechanism is significant. The high local EM field originates from the strong inter-nanorod coupling among close-contacted Au NRs, and therefore the strong SERS signal was obtained. Using the Au NRs films as substrates, a

high success rate in the fabrication of SERS substrates was obtained. In a parallel experiment, about 60% of samples get SERS enhancement. The use of our NRs multilayer films as SERS substrates have several advantages, such as high stability and reliability, as well as high SERS intensity resulted from the unique high density of Au NRs.

#### 4. Conclusions

In this paper, Au NRs multilayered nanostructure has been constructed on the LPEI-functionalized ITO substrate using the layer-by-layer assembly technique. The negatively charged polyelectrolyte PSS was used as a glue molecule of the interlayer Au NRs. By alternately deposition of the PSS and Au NRs on the substrate, high coverage density of Au NRs on the ITO substrate was demonstrated. The plasmon property and the NRs coverage density of the NRs multilayer film are tunable by controlling the number of deposition layers. The multilayered nanostructure has been demonstrated to be an active SERS substrate for probing 4-ATP. The strategy presented here to construct three-dimensional nanostructure of Au NRs is quite facile and easy control, which opens up a routeway to the future application of Au NRs in nanodevices as well as in molecular detection.

**Acknowledgment.** The work described here is supported by the National Science Foundation of China (No. 20275037 and 20275036).

#### References and Notes

- (1) Schmid, G.; Chi, L. F. *Adv. Mater.* **1998**, *10*, 515.
- (2) Weller, H. *Angew. Chem., Int. Ed.* **1998**, *37*, 1658.
- (3) Antonietti, M.; Göltner, C. *Angew. Chem., Int. Ed. Engl.* **1997**, *36*, 910.
- (4) Alivisatos, A. P. *Science* **1996**, *271*, 933.
- (5) Link, S.; Mohamed, M. B.; El-Sayed, M. A. *J. Phys. Chem. B* **1999**, *103*, 3073.
- (6) van der Zande, B. M. I.; Bohmer, M. R.; Fokkink, L. G. J.; Schoonenberger, C. *Langmuir* **2000**, *16*, 451.
- (7) Yu, Y.; Chang, S.; Wang, C. R. C. *J. Phys. Chem. B* **1997**, *101*, 6661.
- (8) Nikoobakht, B.; Wang, J.; El-Sayed, M. A. *Chem. Phys. Lett.* **2002**, *366*, 17.
- (9) Nikoobakht, B.; El-Sayed, M. A. *J. Phys. Chem. A* **2003**, *107*, 3372.
- (10) Mohamed, M. B.; Volkov, V.; Link, S.; El-Sayed, M. A. *Chem. Phys. Lett.* **2000**, *317*, 517.
- (11) Jana, N. R.; Gearheart, L.; Obare, S. O.; Murphy, C. J. *Langmuir* **2002**, *18*, 922.
- (12) Cui, Y.; Wei, Q.; Park, H.; Lieber, C. M. *Science* **2001**, *293*, 1289.
- (13) Zhong, Z.; Wang, D.; Cui, Y.; Bockrath, M. W.; Lieber, C. M. *Science* **2003**, *302*, 1377.
- (14) Jin, S.; Whang, D.; McAlpine, M. C.; Friedman, R. S.; Wu, Y.; Lieber, C. M. *Nano Lett.* **2004**, *4*, 915.
- (15) Nikoobakht, B.; Wang, Z. L.; El-Sayed, M. A. *J. Phys. Chem. B* **2000**, *104*, 8635.
- (16) Reiss, B. D.; Mbindyo, J. N. K.; Martin, B. R.; Nicewarner, S. R.; Mallouk, T.; Natan, M. J.; Keating, C. D. *Mater. Res. Soc. Symp.* **2001**, *635*, C6.2.1.
- (17) Mbindyo, J. N. K.; Reiss, B. D.; Martin, B. R.; Keating, C. D.; Natan, M. J.; Mallouk, T. E. *Adv. Mater.* **2001**, *13*, 249.
- (18) Huang, Y.; Duan, X.; Wei, Q.; Lieber, C. M. *Science* **2001**, *291*, 630.
- (19) Kim, F.; Kwan, S.; Akana, J.; Yang, P. *J. Am. Chem. Soc.* **2001**, *123*, 4360.
- (20) Tao, A.; Kim, F.; Hess, C.; Goldberger, J.; He, R.; Sun, Y.; Xia, Y.; Yang, P. *Nano Lett.* **2003**, *3*, 1229.
- (21) Whang, D.; Jin, S.; Lieber, C. M. *Nano Lett.* **2003**, *3*, 951.
- (22) Whang, D.; Jin, S.; Wu, Y.; Lieber, C. M. *Nano Lett.* **2003**, *3*, 1255.
- (23) Gole, A.; Orendorff, C. J.; Murphy, C. J. *Langmuir* **2004**, *20*, 7117.
- (24) Schmitt, J.; Decher, G.; Dressik, W. J.; Brandow, S. L.; Geer, R. E.; Shashidhar, R.; Calvert, J. M. *Adv. Mater.* **1997**, *9*, 61.
- (25) Lvov, Y.; Decher, G.; Sukhorukov, G. *Macromolecules* **1993**, *26*, 5396.
- (26) Cheung, J. H.; Fou, A. F.; Rubner, M. F. *Thin Solid Films* **1994**, *244*, 985.
- (27) Lvov, Y.; Ariga, K.; Ichinohe, I.; Kunitake, T. *J. Am. Chem. Soc.* **1995**, *117*, 6117.
- (28) Feldheim, D. L.; Crabar, K. C.; Natan, M. J.; Mallouk, T. E. *J. Am. Chem. Soc.* **1996**, *118*, 7640.
- (29) Cant, N. E.; Zhang, H.-L.; Critchley, K.; Mykhalyk, T. A.; Davies, G. R.; Evans, S. D. *J. Phys. Chem. B* **2003**, *107*, 13557.
- (30) Liu, Y. J.; Wang, Y. X.; Claus, R. O. *Chem. Phys. Lett.* **1998**, *298*, 315.
- (31) Lahav, M.; Heleg-Shabtai, V.; Wasserman, J.; Katz, E.; Willner, I.; Durr, H.; Hu, Y. Z.; Bossmann, S. H. *J. Am. Chem. Soc.* **2000**, *122*, 11480.
- (32) Shipway, A. N.; Lahav, M.; Blonder, R.; Willner, I. *Chem. Mater.* **1999**, *11*, 13.
- (33) Nikoobakht, B.; El-Sayed, M. A. *Chem. Mater.* **2003**, *15*, 1957.
- (34) Jana, N. R.; Gearheart, L.; Murphy, C. J. *J. Phys. Chem. B* **2001**, *105*, 4065.
- (35) Johnson, C. J.; Dujardin, E.; Davis, S. A.; Murphy, C. J.; Mann, S. *J. Mater. Chem.* **2002**, *12*, 1765.
- (36) Busbee, B. D.; Obare, S. O.; Murphy, C. J. *Adv. Mater.* **2003**, *15*, 414.
- (37) Cheng, W. L.; Dong, S. J.; Wang, E. K. *Anal. Chem.* **2002**, *74*, 3599.
- (38) Nikoobakht, B.; El-Sayed, M. A. *Langmuir* **2001**, *17*, 6368.
- (39) Malikova, N.; Pastoriza-Santos, I.; Schierhorn, M.; Kotov, N. A.; Liz-Marza'n, L. M. *Langmuir* **2002**, *18*, 3694.
- (40) Gole, A.; Murphy, C. J. *Chem. Mater.* **2005**, *17*, 1325.
- (41) Cant, N. E.; Zhang, H.-L.; Critchley, K.; Mykhalyk, T. A.; Davies, G. R.; Evans, S. D. *J. Phys. Chem. B* **2003**, *107*, 13557.
- (42) Wang, Z.-S.; Sasaki, T.; Muramatsu, M.; Ebina, Y.; Tanaka, T.; Wang, L. Z.; Watanabe, M. *Chem. Mater.* **2003**, *15*, 807.
- (43) Sennerfors, T.; Bogdanovic, G.; Tibergh, F. *Langmuir* **2002**, *18*, 6410.
- (44) Schmitt, J.; Mächtle, P.; Eck, D.; Möhwald, H.; Helm, C. A. *Langmuir* **1999**, *15*, 3256.
- (45) Ung, T.; Liz-Marza'n, L. M.; Mulvaney, P. *J. Phys. Chem. B* **2001**, *105*, 3441.
- (46) Cheng, W. L.; Dong, S. J.; Wang, E. K. *J. Phys. Chem. B* **2004**, *108*, 19146.
- (47) Link, S.; Mohamed, M. B.; El-Sayed, M. A. *J. Phys. Chem. B* **1999**, *103*, 3073.
- (48) Melosh, N. A.; Boukai, A.; Diana, F.; Gerardot, B.; Badolato, A.; Petroff, P. M.; Heath, J. R. *Science* **2003**, *300*, 112.
- (49) Schwartzberg, A. M.; Grant, C. D.; Wolcott, A.; Talley, C. E.; Huser, T. R.; Bogomolni, R.; Zhang, J. Z. *J. Phys. Chem. B* **2004**, *108*, 19191.
- (50) Li, X.; Zhang, J.; Xu, W.; Jia, H.; Wang, X.; Yang, B.; Zhao, B.; Li, B.; Ozaki, Y. *Langmuir* **2003**, *19*, 4285.
- (51) Suzuki, M.; Niidome, Y.; Kuwahara, Y.; Terasaki, N.; Inoue, K.; Yamada, S. *J. Phys. Chem. B* **2004**, *108*, 11660.
- (52) Li, X.; Xu, W.; Zhang, J.; Jia, H.; Yang, B.; Zhao, B.; Li, B.; Ozaki, Y. *Langmuir* **2004**, *20*, 1298.
- (53) Lu, L.; Zhang, H.; Sun, G.; Xi, S.; Wang, H.; Li, X.; Wang, X.; Zhao, B. *Langmuir* **2003**, *19*, 9490.
- (54) Zheng, J.; Li, X.; Gu, R.; Lu, T. *J. Phys. Chem. B* **2002**, *106*, 1019.
- (55) Griffith, W. P.; Koh, T. Y. *Spectrochim. Acta* **1995**, *51*, 253.
- (56) Zheng, J.; Zhou, Y.; Li, X.; Ji, Y.; Lu, T.; Gu, R. *Langmuir* **2003**, *19*, 632.
- (57) Osawa, M.; Matsuda, N.; Yoshii, K.; Uchida, I. *J. Phys. Chem.* **1994**, *98*, 12702.